

 Open  
Access

# Formation of Titanium Dioxide Nanoparticles by Anodization of Valve Metals

Muhammad Syahizul Aidi Berahim<sup>1</sup>, Mohd Fadhil Majnis<sup>\*,1</sup>, Mustaffa Ali Azhar Taib<sup>2</sup>

<sup>1</sup> Department of Chemical and Petroleum Engineering, Faculty of Engineering, Technology & Built Environment, UCSI University, 56000 Kuala Lumpur, Malaysia

<sup>2</sup> Advanced Technology Training Centre (ADTEC) Taiping, PT15643, Kamunting Raya, Mukim Asam Kumbang, 34600 Kamunting, Perak, Malaysia

## ARTICLE INFO

### Article history:

Received 11 November 2018

Received in revised form 1 December 2018

Accepted 1 January 2019

Available online 19 January 2019

### Keywords:

Titanium dioxide nanoparticles,  
Anodization, Annealing, Rutile

## ABSTRACT

TiO<sub>2</sub> nanoparticles (TNPs) were successfully formed by anodization of Ti foil in aqueous (100 mL of Na<sub>2</sub>SO<sub>4</sub>) and an organic (glycerol/H<sub>2</sub>O) electrolyte containing 0.7 g of NH<sub>4</sub>Cl at 20 V for 60 min. The morphology of the formed TNPs was discussed. It was found that TNPs can be formed in both aqueous and organic electrolytes. The diameter of TNPs formed in organic and inorganic solution was generally in the range of 50 nm to 100 nm and the length is in the range of 300 nm to 700 nm. XRD analysis revealed an amorphous phase of the as-anodized sample regardless of the electrolytes used in this work. The thermal annealing at 700 °C indicated the sample dominated by the presence of rutile phase together with anatase phase mixture.

Copyright © 2018 PENERBIT AKADEMIABARU - All rights reserved

## 1. Introduction

Nanotechnology describes the materials, reactions or the process that can be operated at a very small scale (nanoscale). Nanoscale materials are defined as material with at least in one dimension of less than 100 nm. Oxide materials in the form of nanostructured have been investigated due to their novel and various unique properties [1]. Its novel properties have been used in wide-ranging of applications from optoelectronics and semiconductor devices, gas sensors [2, 3], photocatalyst [4], biomedical applications [5], water splitting and energy storage [6]. Among the metal oxide semiconductors mentioned above, the most widely used is titanium dioxide (TiO<sub>2</sub>). TiO<sub>2</sub> or known as titania is a transition metal oxide that presence in three polymorphs in nature: anatase, brookite or rutile [7]. Among these three phases, anatase and rutile have a wider application due to its stability and photoactivity properties compared to brookite.

There are many fabrication methods to synthesize TiO<sub>2</sub>. The formed TiO<sub>2</sub> nanomaterials can be classified based on the dimensionality of their features into zero-dimensional (0-D, nanoparticle), one-dimensional (1-D, nanowire, nanotube or nanorod) and two-dimensional (2-D, nanobelt or nanosheet) [8]. However, it is great interest when it was made in 1-D structure or so-called nanotubular. Typically,

\*Corresponding author.

E-mail address: [fadhil@ucsiuniversity.edu.my](mailto:fadhil@ucsiuniversity.edu.my)

the formation of the nanotubular structure can be produced by the template-assisted method, sol-gel techniques, hydrothermal or anodic oxidation [5, 9]. Among these methods, the formation of nanotubes by anodic oxidation has gained wide interest and much attention since this method has been recognized as an efficient and facile approach to form a vertically-oriented self-ordering nanotubular structure which can be conducted at room temperature [10]. Anodic oxidation or known as anodization is an electrochemical process between anode and cathode that forms an oxide layer on a metal substrate by polarizing the metal anodically in an electrochemical cell.

Other halide ions such as chloride or bromide ions have been reported in the formation of oxide by the anodic oxidation process. To the best of our knowledge, the use of these fluoride-free electrolytes for TiO<sub>2</sub> formation by this method has not yet been explored in great depth. Here we report on the morphology structure evaluation of the anodized Ti in NH<sub>4</sub>Cl added to aqueous and organic electrolyte as anodization electrolyte, respectively. The effect of thermal annealing of formed oxide at high temperature was conducted to investigate the phase formation and transformation. H<sub>2</sub>O has been added in the NH<sub>4</sub>Cl added to glycerol as an oxidant.

## 2. Methodology

Titanium foils (Ti, thickness of 2.0 mm, purity 99.7%, Sigma Aldrich) were cut into 40 x 10 mm and purged by acetone (99.5%, Friendemann Schmidt Chemicals) to clean out any possible grease on its surface, then rinsed with distilled water and dried by an air gun. The experimental work involved five stages: sample preparation, electrolyte preparation, anodization process, heat treatment via thermal annealing and characterization.

In this study, there are two types of electrolytes that were used in a single step of anodization process: (1) aqueous electrolyte of 1 M sodium sulphate (Na<sub>2</sub>SO<sub>4</sub>, 99%, Friendemann Schmidt Chemicals) and (2) organic electrolyte of 85 mL glycerol (C<sub>3</sub>H<sub>8</sub>O<sub>3</sub>, 99.5%, Friendemann Schmidt Chemicals) + 15 mL DI water, making the electrolyte into 100 mL, respectively. Both electrolytes were used 0.7 g ammonium chloride (NH<sub>4</sub>Cl, 99.8%, R&M Chemicals) as an etching agent, respectively. The electrolytes were stirred for 30 min by a magnetic stirrer to ensure the NH<sub>4</sub>Cl salts have fully dissolved and homogeneously mixed. The pH of the aqueous electrolyte was adjusted and controlled in between 3 to 4 therefore for the organic electrolyte, the pH was controlled at 7 (neutral) condition by the addition of 1 M sulfuric acid (H<sub>2</sub>SO<sub>4</sub>, Friendemann Schmidt Chemicals).

The cleaned foils were then immersed in the electrolyte to undergo the electrochemical anodization (single step) process. The Ti foil was used as an anode (working electrode) and the carbon electrode as a cathode (counter electrode). The distance between the two electrodes was kept at ~ 30 mm. Anodisation was performed at 20 V for 60 min using a DC power supply (GP-4303TP, EZ Digital Co. Ltd.) under potentiostatics mode at room temperature. The anodization voltage was continuously ramped-up to the desired potential with a sweep rate of 1 V/s. After anodization process is completed, the as-anodized samples were ultrasonically cleaned in acetone for 30 s and rinse with DI water to remove any surface debris. A schematic diagram of the experimental setup is shown in Fig. 1.

The morphologies of surface and cross-section of anodic samples were observed by field emission scanning electron microscope (FESEM), using an FEI Quanta 200 (FESEM model, USA) at a working distance of around 1 mm. The chemical stoichiometry of the sample was characterized using energy dispersive X-ray (EDX) analysis, which is equipped together with the FESEM. The as-anodized sample was annealed at 700 °C for 3 h. The phase identification of as-anodized and annealed samples was performed using X-ray diffractometer (XRD, Ultima IV, Rigaku RINT 2500). The X-ray source used was Cu K $\alpha$  radiation with  $\lambda = 0.154$  nm and the accelerating voltage was 40 keV at a slow scan step of 0.034° s<sup>-1</sup>. Table 1 shows the parameters set-up for all samples.

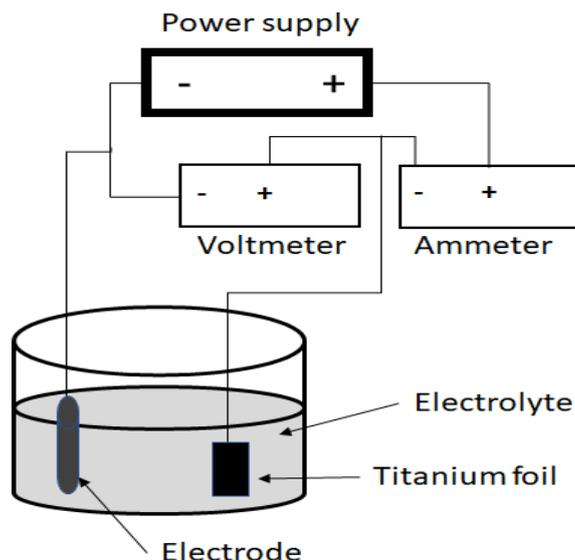


**Fig. 1.** Schematic diagram of the experimental setup for the anodization process

**Table 1** Parameters set-up of the anodization process

Parameter	Sample	
	1	2
Electrolyte type	Aqueous ( $\text{Na}_2\text{SO}_4/\text{NH}_4\text{Cl}$ )	Organic (Glycerol/ $\text{NH}_4\text{Cl}/\text{H}_2\text{O}$ )
Anodization time	60 min	60 min
pH	3 - 4	7
$\text{NH}_4\text{Cl}$ loading	0.7 g	0.7 g
Voltage	20 V	20 V

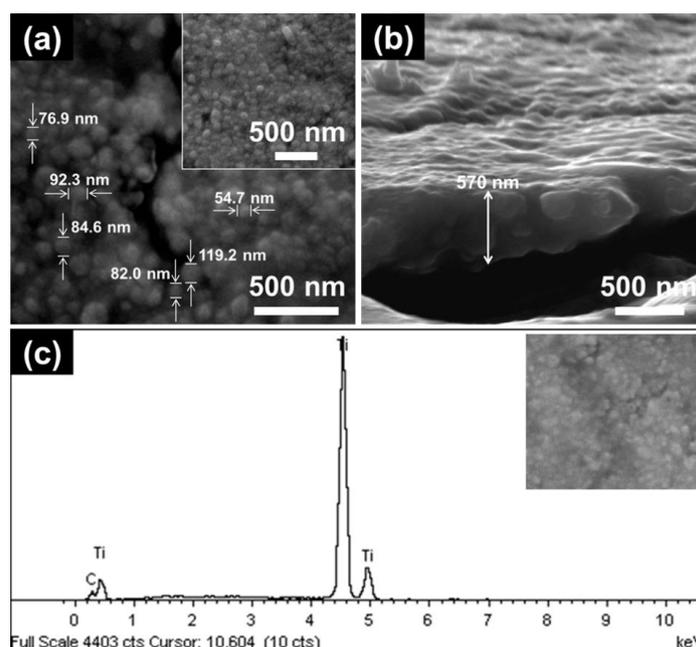
### 3. Results and Discussion

Fig. 2 (a) and (b) are the FESEM images of the anodized Ti in  $\text{Na}_2\text{SO}_4/\text{NH}_4\text{Cl}$  aqueous electrolyte. The small round shape-like structure or termed as  $\text{TiO}_2$  nanoparticles (TNPs) can be seen from the surface morphology of the oxide films (Fig. 2 (a)).

It is clearly seen the diameter of the formed TNPs is non-uniform with an average size of approximately  $\sim 85$  nm. These structures were formed throughout the whole surface of the sample, as seen from the inset image in Fig. 2 (a). Fig. 2 (b) shows the cross-sectional view of the oxide with thickness in the range of 500 nm to 600 nm. Fig. 2 (c) shows the EDX analysis of the anodized Ti. The EDX analysis was conducted to determine the atomic composition of the oxide. EDX shows the titanium and oxygen confirming the formation of  $\text{TiO}_2$ . The presence of carbon in EDX analysis could be due to the post-cleaning process in acetone (which has been used to remove any post-anodizing contamination or to remove any unwanted precipitation salt). From the microscopy images, the formed oxides are indicative of the effectiveness of the anodic process on nanostructures formation on Ti foil.

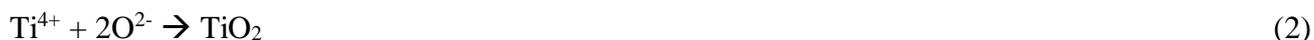
As reported by previous research studies, the smooth feature of the oxide by anodization method could be fabricated by using the organic electrolyte [11, 12]. The use of more viscous organic electrolyte like glycerol caused the  $\text{H}^+$  ions to be retained at the pore bottom. Hence the migration of  $\text{H}^+$  from the pore bottom outwards would be much hindered using this solution. Fig. 3 shows the FESEM images of surface morphology (Fig. 3 (a)) and cross-sectional view (Fig. 3 (b)) of anodic TNPs formed in the organic (glycerol/ $\text{NH}_4\text{Cl}/\text{H}_2\text{O}$ ) electrolyte. Comparing this with TNPs formed in

the aqueous  $\text{Na}_2\text{SO}_4/\text{NH}_4\text{Cl}$  electrolyte, the FESEM images of the formed oxide is cleaner and smoother. The diameter of the TNPs is non-uniform with an average size of 50 nm to 150 nm. Although the TNPs diameter is seen to be increased as compared to aqueous derived samples, the thickness of the formed oxide in glycerol/ $\text{NH}_4\text{Cl}/\text{H}_2\text{O}$  electrolyte is rather thin;  $\sim 255$  nm as observed from the cross-sectional view (Fig. 3 (b)). It is anticipated that 20 V of applied voltage is considered relatively low to accelerate the chemical dissolution process in organic electrolyte hence it produces thinner oxide compared to aqueous electrolyte. Fig. 3 (c) is the EDX analysis of TNPs that shows the oxygen and titanium content confirming the formation of  $\text{TiO}_2$  with the presence of carbon content. The presence of carbon content in this as-anodized sample is rather similar as mentioned in the previous discussion for sample fabricated in  $\text{Na}_2\text{SO}_4/\text{NH}_4\text{Cl}$  aqueous electrolyte (Fig. 2 (c)).



**Fig. 2.** FESEM images of as-anodized sample formed at 20 V for 60 min in 1 M  $\text{Na}_2\text{SO}_4/\text{NH}_4\text{Cl}$  electrolyte: (a) surface morphology (inset: low magnification), (b) cross-sectional view; and EDX analysis (inset: spot area) and (c) EDX analysis of the anodized Ti

The growth of oxide at the surface of the Ti metal is due to the interaction of metallic cations ( $\text{Ti}^{4+}$ ) with  $\text{O}^{2-}$  species coming from  $\text{H}_2\text{O}$  dissociation (Eq. 2) [13]. Once the  $\text{TiO}_2$  initial layer is formed, the activity is controlled by the electric field within the oxide layer for the  $\text{Ti}^{4+}$  outwards migration and the  $\text{O}^{2-}$  inward migration [14]. Hydrogen evolution occurred at the cathode (Eq. 4). This reaction happens rapidly during the early stage of the anodization process. Then with the growth of the oxide barrier layer, resistance increases and reaction speed decreases. The overall reactions are explained as:



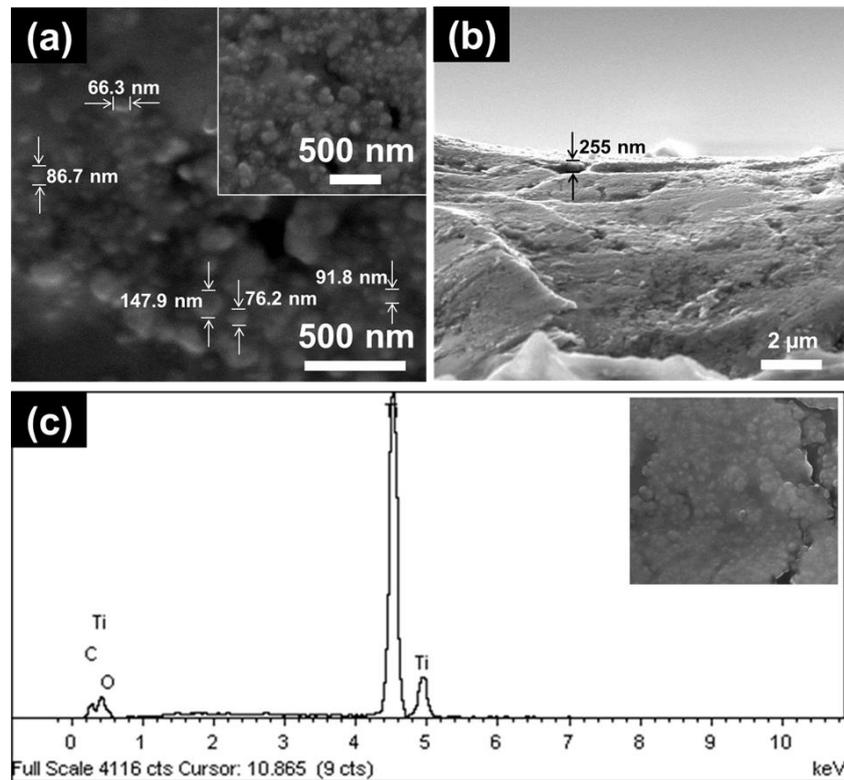


**Fig. 3.** FESEM images of as-anodized sample formed at 20 V for 60 min in glycerol/ $\text{NH}_4\text{Cl}/\text{H}_2\text{O}$  electrolyte: (a) surface morphology (inset: low magnification), (b) cross-sectional view; and EDX analysis (inset: spot area) and (c) EDX analysis of TNPs

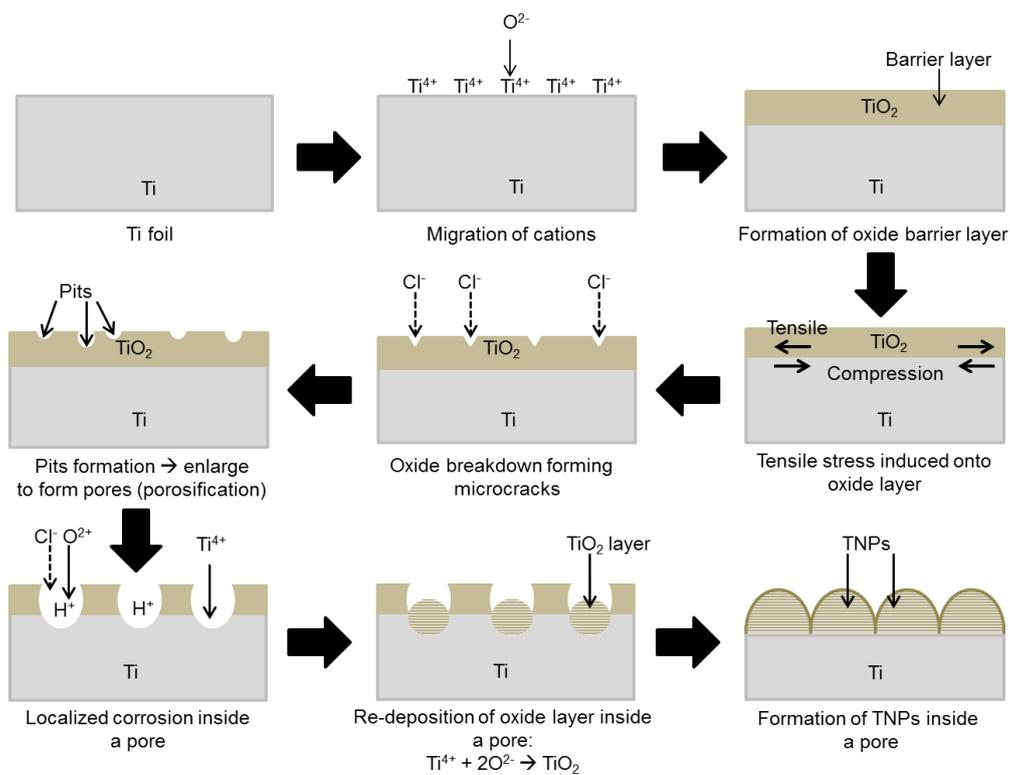


**Fig. 4.** Mechanism of TNPs structure formation in both aqueous and organic electrolytes

With the generation of the TiO<sub>2</sub> film, the volume must expand at the surface of the Ti metal due to the inward migration of O<sup>2-</sup> into Ti. Then volume expansion and distortion of lattice become greater and reaction heat becomes more difficult to be released. In order to lower the internal stress, a huge number of microcracks arise on the oxide|electrolyte interface. The small cracks will be quickly filled by the electrolyte. The chemical etching will occur making the cracks larger and developed into pits especially when chloride ions are present. Moreover, one may expect the incorporation of Cl<sup>-</sup> ions into TiO<sub>2</sub> lattice. This reaction of electrochemical dissolution resulted in the formation of soluble chloro-complexes (titanium hexachloride, [TiCl<sub>6</sub>]<sup>2-</sup>) can be described as follows:



Pits grow-up with time, forming larger and more stable pores. On the other hand, it provides an easier pathway for more O<sup>2-</sup>, OH<sup>-</sup> or Cl<sup>-</sup> to migrate through the barrier layer, leading to further metal oxidation. Furthermore, due to the occurrence of microcracks, the electric field distribution within the oxide film changes. Especially at the bottom of the cracks, field increases greatly and porosification process happens due to the accumulation of H<sup>+</sup> ions inside the pores bottom (local acidification) [15]. pH of the electrolyte at the pore bottom will be reduced, accelerating the chemical dissolution process in here. Due to this, pores should have grown inwards to form the typical elongated pore structure.

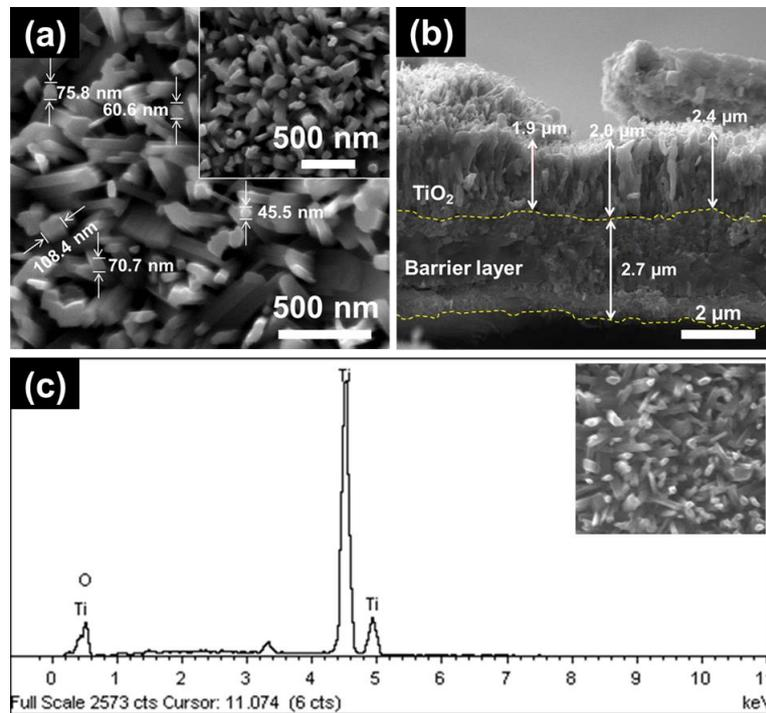
However, for the case of chloride electrolyte such structure is absent [16]. The possible explanation is the extremely rapid oxidation process of Ti with the presence of Cl<sup>-</sup> ions. It may have induced the release of Ti<sup>4+</sup> in the electrolyte and upon reacting with O<sup>2-</sup> ions, it would form TiO<sub>2</sub>. The oxide is however understood to have been precipitated on the surface of the Ti metal instead of being incorporated within the lattice of the parent metal. This could be due to the release of oxygen bubbles during the process of oxidation which decreases the growth efficiency of the oxide. The deposition of the new oxide layer occurs inside a pore and the layers were built up from the oxidation process. As fewer ions are released due to oxide growth and it became taller, the top part of the structure is more pointed forming particle like-structure from the top view. The pores are thought to be the “template” for the TNPs to form and grow. Nonetheless, more experimental variation and characterization are needed in investigating why the TNPs structure formed on Ti when it is anodized in chloride electrolyte.

Fig. 5 shows the FESEM images of (a) surface morphology and (b) cross-sectional view of the oxide subjected to annealing at 700 °C in the air. The high temperature of thermal annealing for 3 h has changed the TNPs structure into nanorod structure due to thermal oxidation process as clearly shown in Fig. 5 (a) from the top view. The average diameter of the rods approximately 72 nm.

As shown in Fig. 5 (b), the length of the oxide approximately 4.5 μm to 5 μm. Moreover, Fig. 5 (c) shows the EDX spectra of the TNPs that shows the oxygen and titanium which confirming the formation of TiO<sub>2</sub> that underwent the annealing process at 700 °C. Due to the thermal oxidation process, rutile protrusion on the parent metal is observed. The detection of rutile is not only due to the phase transformation, however it also because of the excessive grain growth process. This is proved from the surface morphology of the sample in Fig. 5 (b), where new oxide emerges from the oxide surface. A similar observation was also mentioned by Grimes and Mor [17]. Furthermore, provided with a high temperature of thermal annealing at 700 °C, it increases the oxidation of Ti metal substrate. Ti<sup>4+</sup> diffuses from the Ti metal substrate outwards to the oxide|air interface [18]. The thermal oxidation leads to the annihilation of the TNPs structure due to the excessive growth of the oxide rapidly. Consequently, the bottom part of the oxide (barrier layer) becomes thicker and form as compact oxide.

XRD analysis was carried out to investigate the effect of heat treatment on the phase formation of the TNPs. Fig. 6 shows the XRD pattern of samples before and after thermal annealing. XRD pattern

of Ti foil is also shown. The as-anodized sample was found to be amorphous given that only Ti peaks (ICSD No. 96-900-8518) at  $2\theta$ :  $35.0^\circ$ ,  $38.4^\circ$ ,  $40.1^\circ$ ,  $53.0^\circ$ ,  $62.9^\circ$  and  $70.6^\circ$  are seen.



**Fig. 5.** FESEM images: (a) surface morphology (inset: low magnification) and (b) cross-sectional view); and (c) EDX analysis (inset: spot area) of annealed TNPs at  $700^\circ\text{C}$  for 3 h in air fabricated in 1 M  $\text{Na}_2\text{SO}_4$  electrolyte at 20 V for 60 min

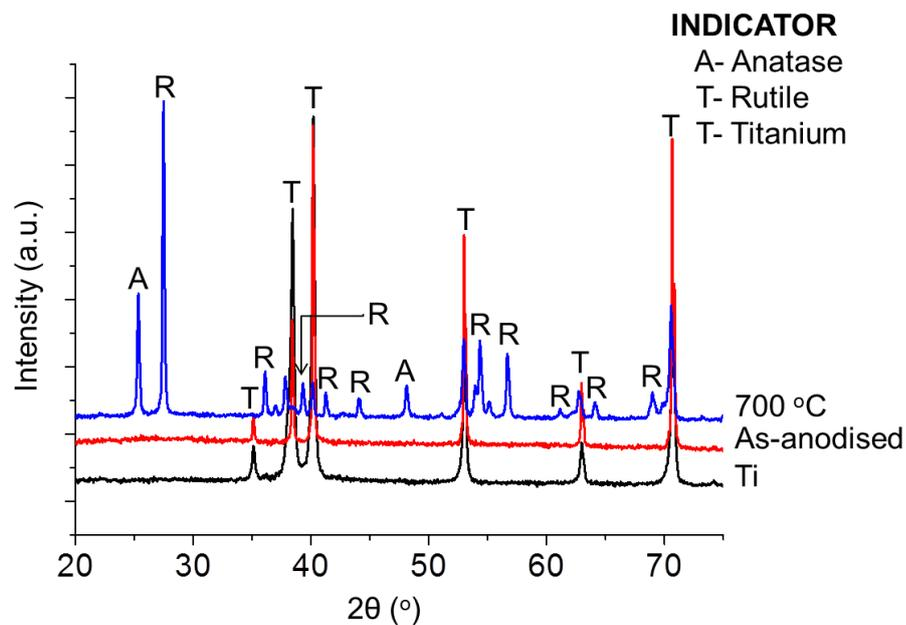


**Fig. 6.** XRD patterns of Ti foil, as-anodised and annealed TNPs at  $700^\circ\text{C}$  for 3 h in air fabricated in 1 M  $\text{Na}_2\text{SO}_4$  electrolyte at 20 V for 60 min

As seen from the Fig. 6, the formation of anatase and rutile phases can be detected when the sample was subjected to heat at 700 °C [19]. It is obvious that rutile peaks with higher intensity are dominating at  $2\theta$ : 27.5 °, 36.0 °, 39.2 °, 41.2 °, 44.0 °, 54.3 °, 56.6 °, 64.0 ° and 69.0 °; and remaining of anatase peaks still can be observed at  $2\theta$ : 25.3 ° and 48.0 °. Rutile crystals can be formed due to the oxidation of Ti foil or due to the phase transformation from anatase crystals. Fang et al suggested that the Ti substrate promoted the anatase to rutile transition when oxide situated on a Ti foil above 600 °C [20]. During the nucleation of rutile from anatase, the crystallites may rotate and re-orient [20] to get the best crystallographic matching if sufficient volume is available.

Furthermore, the transformation of anatase to rutile involves the breaking and reforming of bonds [21]. This process is attributed to the cooperative arrangement of  $Ti^{4+}$  and  $O^{2-}$  ions within the planes which occur at high temperature [22]. The Ti peaks are also observed which belong to Ti metal underneath the oxide layer for annealed TNPs sample.

#### 4. Conclusion

By anodization of valve metals, TNPs has been successfully formed on Ti metal foil. It was found that oxide can be formed in both aqueous and organic electrolyte. The diameter size of TNPs formed in organic and inorganic electrolytes was generally in the range of 50 nm to 100 nm and the length is in the range of 200 nm to 600 nm. However, when the as-anodized sample undergoes the annealing process, the morphology of TNPs has transformed to nanorods structure due to thermal oxidation process of Ti metal foil. The oxide thickness of the annealed sample was about 4500 nm to 5000 nm. Detailed analysis of annealing on TNPs reveals that phase formation of anatase and rutile mixture, with rutile phase dominated at 700 °C. Further study needs to be done on different annealing temperatures in order to study the phase formation and transformation of anatase to rutile crystals in detail. The morphology evolution of TNPs to nanoporous or nanotubes structure can be determined by altering the composition of electrolytes, introduction of an oxidant, variation of applied voltage, tuning of pH and concentration of electrolyte and few other factors.

#### Acknowledgement

The authors gratefully acknowledge the Centre of Excellence for Research, Value Innovation and Entrepreneurship (CERVIE), UCSI University, Malaysia for funding this work under PSIF grant (Proj-In-FETBE-037).

#### References

- [1] Ahmadi, E., Azhar, M. A., Anwar, D. M., Rozana, M. and Lockman, Z. "The effect of crystallinity of nanoporous  $WO_3$  on the intercalation and deintercalation of  $Li^+$ ." in *Advanced Materials Research* (2014). Trans Tech Publication.
- [2] Sun, Y.-F., Liu, S. B., Meng, F. L., Liu, J. Y., Jin, Z., Kong, L. T. and Liu, J. H. "Metal oxide nanostructures and their gas sensing properties: a review." *Sensors* 12 (2012): 2610-2631.
- [3] Li, Y., X. Yu, and Q. Yang, "Fabrication of nanotube thin films and their gas sensing properties". *Journal of Sensors* (2009): Article ID 402174.
- [4] Smith, Y., Ray, R., Carlson, K., Sarma, B. and Misra, M. "Self-ordered titanium dioxide nanotube arrays: anodic synthesis and their photo/electro-catalytic applications." *Materials* 6 (2013): 2892-2957.
- [5] Kulkarni, M., Mazare, A., Gongadze, E., Perutkova, S., Kralj-Iglic, V., Milosev, I. and Mozetic, M. "Titanium nanostructures for biomedical applications." *Nanotechnology* 26 (2015): p. 062002.
- [6] Jafari, T., Moharreri, E., Amin, A. S., Miao, R., Song, W. and Suib, S. L. "Photocatalytic water splitting-the untamed dream: a review of recent advances." *Molecules* 21 (2016): 900.
- [7] Hanaor, D.A. and C.C. Sorrell "Review of the anatase to rutile phase transformation." *Journal of Materials Science* 46 (2011): 855-874.
- [8] Pokropivny, V. and V. Skorokhod, "New dimensionality classifications of nanostructures." *Physica E: Low-dimensional Systems and Nanostructures* 40 (2008): 2521-2525.
- [9] Ge, M., Li, Q., Cao, C., Huang, J., Li, S., Zhang, S. and Lai, Y. "One-dimensional  $TiO_2$  nanotube photocatalysts for solar water splitting." *Advanced Science* 4 (2017): 1600152.

- [10] Ge, M. Z., Cao, C.Y., Huang, J. Y., Li, S. H., Zhang, S. N., Deng, S. and Lai, Y. K. "Synthesis, modification, and photo/photoelectrocatalytic degradation applications of TiO<sub>2</sub> nanotube arrays: a review." *Nanotechnology Reviews* 5 (2016): 75-112.
- [11] Macak, J.M., Tsuchiya, H., Taveira, L., Aldaberrgerova, S. and Schmuki, P. "Smooth anodic TiO<sub>2</sub> nanotubes". *Angewandte Chemie International Edition* 44 (2005): 7463-7465.
- [12] Paulose, M., Prakasam, H. E., Varghese, O. K., Peng, L., Papat K. C. Mor, G. K. and Grimes, C. A. "TiO<sub>2</sub> nanotube arrays of 1000 μm length by anodization of titanium foil: phenol red diffusion." *The Journal of Physical Chemistry C* 111 (2007): 14992-14997.
- [13] Su, Z. and W. Zhou, "Formation, morphology control and applications of anodic TiO<sub>2</sub> nanotube arrays." *Journal of Materials Chemistry* 21 (2011): 8955-8970.
- [14] Taib, M.A.A., Tan, W. K., Okuno, T., Kawamura, G., Jaafar, M., Razak, K. A. and Lockman, Z. "Formation of TiO<sub>2</sub> nanotube arrays by anodic oxidation in LiOH added ethylene glycol electrolyte and the effect of thermal annealing on the photoelectrochemical properties" in *AIP Conference Proceedings*. (2016). AIP Publishing.
- [15] Lockman, Z., Ismail, S., Sreekantan, S., Schmidt-Mende, L. and MacManus-Driscoll, J. L. "The rapid growth of 3 μm long titania nanotubes by anodization of titanium in a neutral electrochemical bath." *Nanotechnology* 21 (2009): 055601.
- [16] Bashirrom, N., Razak, K. A., Yew, C. K., & Lockman, Z. "Effect of fluoride or chloride ions on the morphology of ZrO<sub>2</sub> thin film grown in ethylene glycol electrolyte by anodization." *Procedia Chemistry* 19 (2016): 611-618.
- [17] Grimes, C.A. and G.K. Mor, "TiO<sub>2</sub> nanotube arrays: synthesis, properties, and applications." (2009): Springer Science & Business Media.
- [18] Lockman, Z., C.H. Kit, and S. Sreekantan, "Effect of annealing temperature on the anatase and rutile TiO<sub>2</sub> nanotubes formation." *Journal Nuclear and Related Technologies* 6 (2009): p. 57-64.
- [19] Taib, M.A.A., Razak, K. A., Jaafar, M. and Lockman, Z. "Initial growth study of TiO<sub>2</sub> nanotube arrays anodised in KOH/fluoride/ethylene glycol electrolyte." *Materials & Design*,128 (2017): p. 195-205.
- [20] Fang, D., Luo, Z., Huang, K. and Lagoudas, D.C. "Effect of heat treatment on morphology, crystalline structure and photocatalysis properties of TiO<sub>2</sub> nanotubes on Ti substrate and freestanding membrane." *Applied Surface Science* 257 (2011): 6451-6461.
- [21] Oi, L.E., Choo, M. Y., Lee, H. V., Ong, H. C., Hamid, S. B. A. and Juan, J. C. "Recent advances of titanium dioxide (TiO<sub>2</sub>) for green organic synthesis." *RSC Advances* 6 (2016): 108741-108754.
- [22] Shannon, R.D. and J.A. Pask, "Kinetics of the anatase-rutile transformation." *Journal of the American Ceramic Society* 48 (1965): 391-398.